ChemPubSoc Europe

DOI: 10.1002/cphc.201402774

CHEMPHYSCHEM Articles

Enhancement of Photophysical and Photosensitizing Properties of Flavin Adenine Dinucleotide by Mutagenesis of the C-Terminal Extension of a Bacterial Flavodoxin Reductase

Lorena Valle,[a] Inés Abatedaga,[a] Faustino E. Morán Vieyra,[a] Ana Bortolotti,[b] Néstor Cortez,*[b] and Claudio D. Borsarelli*[a]

The role of the mobile C-terminal extension present in *Rhodobacter capsulatus* ferredoxin–NADP(H) reductase (*Rc*FPR) was evaluated using steady-state and dynamic spectroscopies for both intrinsic Trp and FAD in a series of mutants in the absence of NADP(H). Deletion of the six C-terminal amino acids beyond Ala266 was combined with the replacement A266Y to emulate the structure of plastidic reductases. Our results show that these modifications of the wild-type *Rc*FPR produce subtle global conformational changes, but strongly reduce the local rigidity of the FAD-binding pocket, exposing the isoalloxazine ring to the solvent. Thus, the ultrafast charge-transfer quenching of ^{1}FAD* by the conserved Tyr66 residue was absent in the mutant series, producing enhancement of the excited singlet- and triplet-state properties of FAD. This work highlights the delicate balance of the specific interactions between FAD and the surrounding amino acids, and how the functionality and/or photostability of redox flavoproteins can be modified.

1. Introduction

Ferredoxin (or flavodoxin)–nicotinamide adenine dinucleotide phosphate [NADP(H)] reductases (FNRs) are monomeric enzymes located in several organisms and tissues that attach the flavin adenine dinucleotide (FAD) noncovalently as a prosthetic group. These flavoenzymes mediate the electron-transfer (ET) chains implicated in diverse metabolic processes such as photosynthesis, nitrogen fixation, isoprenoid biosynthesis, steroid metabolism, xenobiotic detoxification, oxidative-stress response, and iron–sulfur cluster biogenesis, by catalyzing the reversible ET between one molecule of NADP(H) and two molecules of the low-potential electron-carrier proteins ferredoxin or flavodoxin. The overall reaction can be separated into a hydride-transfer step between NADP(H) and FAD, and an electron-exchange reaction between FAD and the electron-carrier protein partner.[1] Both sequence and structural analysis of plant-type FNRs led to subdivision of the family into two classes: the plastidic-class, consisting of proteins present in cyanobacteria and in chloroplasts from plants and algae, and bacterial-class —known as FPRs—present in eubacteria.[1c,d] The impact on the catalytic efficiency of both types of reductases by changes on the amino acid sequence and architecture of the C-terminal region belonging to the NADP(H)-binding domain, has been reviewed.[1,2] In a recent report, the role of the mobile C-terminal extension during catalysis of the FPR of *Rhodobacter capsulatus* (*Rc*FPR) was analyzed by deletion of the hexapeptide beyond Ala266 (Δ=FVGEGI) and in combination with the replacement of Ala266 by Tyr, emulating the structure present in plastidic versions of these flavoenzymes.[2b] Although the changes in the C-terminal domain did not significantly alter the global structure of the protein, they promoted the thermal instability of the mutants and also prevented the optimal geometry of the active FAD–NADP(H) charge-transfer (CT) complex being achieved. The decreased catalytic rate parameters confirmed that hydride transfer from NADPH to the flavin ring is considerably impeded in all C-terminal mutants as compared with the wild-type (WT) *Rc*FPR. Furthermore, all *Rc*FPR variants displayed higher affinity for $NADP^+$ than the WT, evidence of the contribution of the C terminus in tempering a non-productive strong (rigid) interaction with the coenzyme.[2] In addition, preliminary absorbance and fluorescence spectral analysis of FAD for the *Rc*FPR mutants suggested that the C-terminal modification does not greatly change the general geometry of the FAD binding site, but increases the exposure of the flavin isoalloxazine ring to the solvent.[2b]

All naturally occurring flavins are derivatives of the nitrogen heterocycle 7,8-dimethylisoalloxazine, and have the capability to transfer up to $2H^+/2e^-$.[3] The fully oxidized form of the isoalloxazine ring absorbs intensely electromagnetic radiation between the UVA and blue–visible region (320–480 nm), showing green fluorescence emission and efficient formation of a triplet

[a] Dr. L. Valle, Dr. I. Abatedaga, Dr. F. E. M. Vieyra, Prof. Dr. C. D. Borsarelli
Centro de Investigaciones y Transferencia de
Santiago del Estero (CITSE-CONICET)
Universidad Nacional de Santiago del Estero
RN9 Km 1125. 4206, Santiago del Estero (Argentina)
E-mail: cdborsarelli@gmail.com

[b] Dr. A. Bortolotti, Prof. Dr. N. Cortez
Instituto de Biología Molecular y Celular de Rosario (IBR-CONICET)
Universidad Nacional de Rosario
Suipacha 531, S2002LRK, Rosario (Argentina)
E-mail: cortez@ibr-conicet.gov.ar

excited state.[4] The latter long-lived excited state is also able to react with triplet molecular oxygen ($^3O_2$) by both CT and energy-transfer quenching processes to generate radical ions and neutral reactive species, such as the superoxide anion ($O_2^{\bullet-}$) and singlet molecular oxygen ($^1O_2$), respectively.[4]

The photons absorbed by the flavin cofactor in light-inducible flavoproteins are transduced into a biochemical signal to modulate the physiological activities of plants, algae and bacteria.[5] In contrast, redox flavoproteins require efficient quenching mechanisms of the excited states of the flavin cofactors to avoid deleterious effects produced by either primary or secondary photoinduced reactive species.[6] The genetic engineering of the structure of a flavoprotein can modify the surrounding nano-environment of the flavin, resulting in the enhancement of its photophysical properties, such as increased green fluorescence emission and generation of a long-lived excited triplet state that, under aerobic conditions, can also photosensitize $^1O_2$.[7]

In the present work, we evaluated the impact of modifying the C-terminal tail on the spectroscopic and photophysical properties of FAD bound to several variants of *Rc*FPR in the absence of NADP(H) (Figure 1). The steady-state and dynamic behavior of both the intrinsic Trp and cofactor fluorescence was analyzed, as well as the formation of the excited triplet state of the flavin and its interaction with $^3O_2$ to generate $^1O_2$. The results presented here confirmed that C-terminal modification of the native *Rc*FPR enhances the formation of both singlet and triplet excited states of the bound flavin, mainly due to conformational changes in the FAD-binding domain.

2. Results

2.1. UV/Vis Spectral Changes

Some general steady-state spectroscopic features of the *Rc*FPR variants indicated in Figure 1 were recently presented by Bortolotti et al.[2b] In this work, we studied in more detail both spectroscopic and photophysical features of the *Rc*FPR series. Figure 2 shows a comparison of the UV/Vis absorption spectra of free FAD with both WT and A266YΔ enzymes in Tris buffer (50 mM pH 8). For the rest of the enzymes (data not shown),

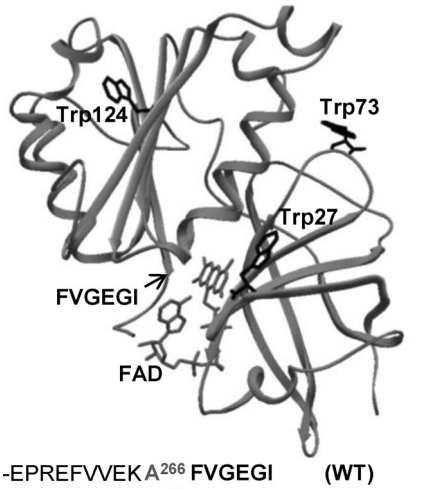

Figure 1. 3D crystal structure of WT *Rc*FPR (PDB ID: 2BGJ; MW = 33 kDa), indicating the configuration of the FAD cofactor, Trp residues, and the C-terminal FVGEGI tail that was modified in different mutants.

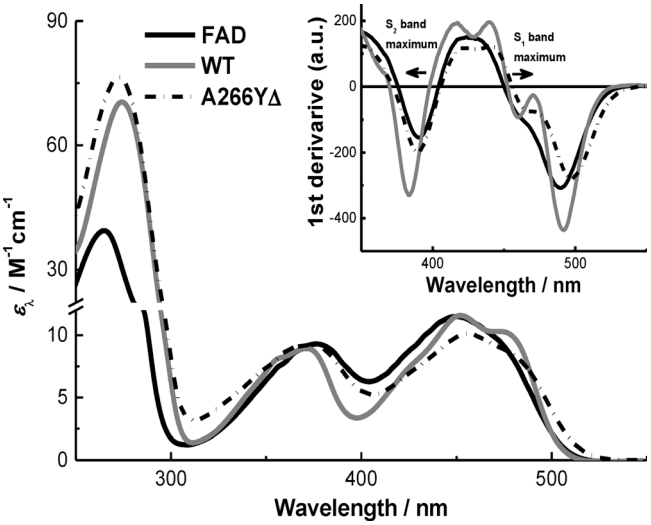

Figure 2. UV/Vis absorption spectra of FAD and WT and A266YΔ *Rc*FPR enzymes in Tris buffer (50 mM, pH 8). Inset: First-derivative spectra indicating the direction of the spectral shift of each visible band.

the two characteristic intense $\pi \rightarrow \pi^*$ absorption bands of the fully oxidized isoalloxazine ring are also present, corresponding to the transitions from the ground state (S_0) to the lowest-lying excited states of the singlet manifold S_1 ($\lambda_{max} \approx 442$–450 nm) and S_2 ($\lambda_{max} \approx 360$–375 nm).[4] The molar absorption coefficient at the maximum ($\varepsilon_\lambda^{max}$) of the S_1 band in the WT and A266Δ was closer to that of free flavin in buffer solution, although the two variants with an extra Tyr in the NADP(H)-binding domain—A266Y and A266YΔ—showed smaller $\varepsilon_\lambda^{max}$ values (Table 1). Instead, the UV band of the isoalloxazine ring observed in buffer at around 264 nm was overlapped and red-shifted for all *Rc*FPR variants by the sum of the absorbance of the Tyr and Trp residues present in the enzymes. In the case of both A266Y and A266YΔ, the $\varepsilon_\lambda^{max}$ value of the UV band was slightly larger than for the enzymes lacking this extra Tyr residue, due to its contribution to the total absorbance in the region around 275 nm ($\varepsilon_{275}^{Tyr} \approx 1500\ M^{-1}cm^{-1}$).

The general effect of the enzyme on the absorption bands of FAD is comparable to that observed for free flavins in less polar and/or hydrogen-bonding media, and/or by local rigidity imposed on the isoalloxazine ring, as the S_2 band is generally shifted to shorter wavelengths and the S_1 band splits into extra vibrational transition bands.[4,8] To cancel out possible scattering effects on the absorption spectra of the enzyme solutions, the first-derivative spectra of the S_1 and S_2 bands of the flavin were compared (Figure 2, inset), and the same trend was observed. In particular, the spectra of all *Rc*FPR enzymes show a hyperchromic effect at the red edge of the S_1 absorption band of the flavin with a well-defined vibrational shoulder at

Table 1. UV/Vis absorption properties of FAD and *Rc*FPR enzymes in Tris buffer (50 mM, pH 8) at 25 °C.[a]

	λ_{max} [nm]			$\varepsilon_{\lambda}^{max}$ [mM^{-1} cm^{-1}]			
	UV	S_2	S_1	UV	S_2	S_1	A_{480}/A_{450}
WT	274	370	452	75.2	9.0	11.7	0.89
A266Y	268	374	456	79.0	10.1	10.1	0.85
A266YΔ	272	373	456	77.3	9.3	9.7	0.83
A266Δ	268	373	455	75.0	9.8	11.3	0.81
FAD	264	376	450	39.1	9.3	11.5	0.70

[a] Experimental error $\leq$5%.

approximately 480 nm, increasing the absorption ratio A_{480}/A_{450} for the enzymes in comparison with the free flavin (Table 1). This vibronic (i.e. vibrational and electronic) enhancement is a common feature of FAD-bearing enzymes, such as NADH peroxidase,[9] and thioredoxin[8a] and glutathione[10] reductases, all of which contain the conserved aromatic amino acid residues Tyr or Trp close (e.g. $<$5 Å) to the isoalloxazine ring, with proper orientation. In fact, the same spectral effect has been also observed for model flavinyl–tryptophan and flavinyl–tyrosine intramolecular complexes.[11]

2.2. Changes in Intrinsic Enzyme Fluorescence

Figure 3a shows the normalized steady-state fluorescence emission spectra of free Trp, and the intrinsic Trp emission of both WT and A266YΔ enzymes in air-saturated buffer solutions obtained by excitation at 295 nm. The main fluorescence emission properties are summarized in Table 2. The structureless and slightly red-shifted fluorescence spectra of the modified *Rc*FPR contrast with that of the WT enzyme with $\lambda_F^{max} = 323$ nm and a small shoulder at approximately 330 nm. The position of the Trp emission band in proteins is somewhat sensitive to its local environment, with λ_F^{max} values ranging from 308 (azurin) to 355 nm (e.g. glucagon), which approximately correlates with the degree of solvent exposure of the residue.[12] As the *Rc*FPR enzymes contain three Trp residues at positions 27, 73, and 124 (Figure 1), the intrinsic blue-shifted and narrower emission

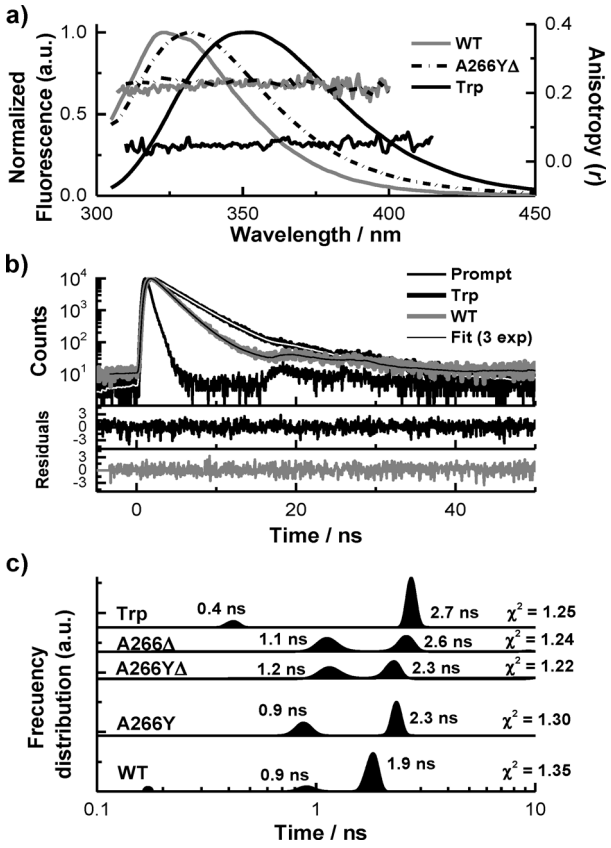

Figure 3. a) Normalized fluorescence emission spectra of WT and A266YΔ *Rc*FPR and Trp in air-saturated Tris buffer (50 mM, pH 8), with excitation at 295 nm, corrected by primary and secondary inner filter effects produced by the cofactor FAD, together with the respective emission anisotropy *r*. b) Fluorescence emission decay of WT *Rc*FPR and Trp, obtained with NanoLED excitation at 280 nm and monitored at 325 and 350 nm, respectively, together with the fitting curves obtained by deconvolution using a three-exponential decay function. c) Trp-like lifetime distributions of the *Rc*FPR variants obtained by decay analysis with the hybrid ME/NLS algorithm (MemExp, version 4.0).[13]

Table 2. Steady-state and dynamic parameters of the Trp-like fluorescence of *Rc*FPR variants in air-saturated Tris buffer (50 mM, pH 8).[a]

	λ_F [nm]	FWHM [nm]	Φ_F ($\times 10^2$)	r[b]	τ_1 [ns] (%f_1)	τ_2 [ns] (%f_2)	τ_3 [ns] (%f_3)	τ_F [ns]	χ^2
WT	323	48.7	7.0	0.221	1.09 (17)	1.84 (80)	6.31 (3)	1.86	1.021
A266Y	327	52.9	7.9	0.233	0.80 (17)	2.18 (70)	5.31 (13)	2.33	1.109
A266YΔ	330	53.1	7.3	0.231	0.56 (5)	1.70 (75)	4.64 (20)	2.22	1.112
A266Δ	331	56.5	11.2	0.215	0.97 (21)	2.16 (60)	5.11 (19)	2.46	1.047
Trp	350	64.0	14.0	0.065	0.54 (3)	2.77 (90)	7.86 (7)	3.03	1.036

[a] Experimental error $\leq$5%. [b] Value at the emission maximum.

of the enzymes suggests that the emitting amino acids are partially buried and/or excluded from interacting with water molecules. In addition, the fluorescence quantum yield Φ_F of the enzyme was slightly lower than that of Trp in buffer, suggesting an environmental quenching effect of the enzyme. Finally, the steady-state anisotropy *r* associated with the Trp emission of the *Rc*FPR enzymes was almost threefold larger than that of free Trp in solution (Figure 3a), indicating a large hindrance of the segmental motion of the emitting Trp indole moiety in the enzymes.

In turn, Figure 3b shows a comparison of the fluorescence emission decays of WT *Rc*FPR and free Trp in air-saturated buffer solutions obtained using the time-correlated single-photon counting (TCSPC) technique with pulsed excitation at 280 nm and detection at 325 and 350 nm, respectively. In all cases, the Trp emission decays were satisfactorily fitted with a three-exponential component function,[12a] for which the individual decay time τ_i and fractional con-

tribution f_i of each decay time to the steady-state intensity are listed in Table 2, together with the average lifetime calculated as $\tau_F = \Sigma f_i \tau_i$, as described elsewhere.[12a] The analyzed fluorescence decay data indicated that C-terminal modification of WT *Rc*FPR produces subtle changes on both the fractional contribution and component lifetimes, resulting in a small enlargement of the average fluorescence lifetime τ_F for the enzyme variants (Table 2).

The impact of enzyme modification on the behavior of the intrinsic fluorescence decay can be also visualized by performing a lifetime distribution analysis of the fluorescence decays using the hybrid maximum-entropy/nonlinear least squares (ME/NLS) algorithm of the software package MemExp (version 4.0; see equations in Steinbach et al.[13] and references therein). The ME/NLS analysis recovered up to three kinetic processes, but only the contribution of the shorter and middle lifetime populations were significant (Figure 3c), probably due to the spreading of statistical error of the last portion of the decay tail. As compared with the WT enzyme, the *Rc*FPR variants showed a slightly different lifetime distribution, with progressive shifting to longer lifetime values and more similar relative contribution for both lifetime populations.

2.3. Cofactor Fluorescence Behavior

Figure 4a shows the normalized steady-state fluorescence emission spectra of free FAD and bound in WT and A266YΔ *Rc*FPR enzymes in air-saturated buffer, obtained by excitation at 450 nm. The cofactor bound to the WT enzyme showed the largest blue-shift and narrower band emission, together with the lowest Φ_F and largest *r* values (Table 3). In contrast, all modified *Rc*FPR enzymes showed similar emission parameters to that observed for the free flavin in buffer solution. These results suggest that the environmental properties sensed by the isoalloxazine ring of FAD bound to the modified enzymes are similar to those in bulk solvent. However, this last result seems somewhat incongruous with FAD–enzyme interactions interpreted from the vibronic structure of the S_1 absorption band as described above.

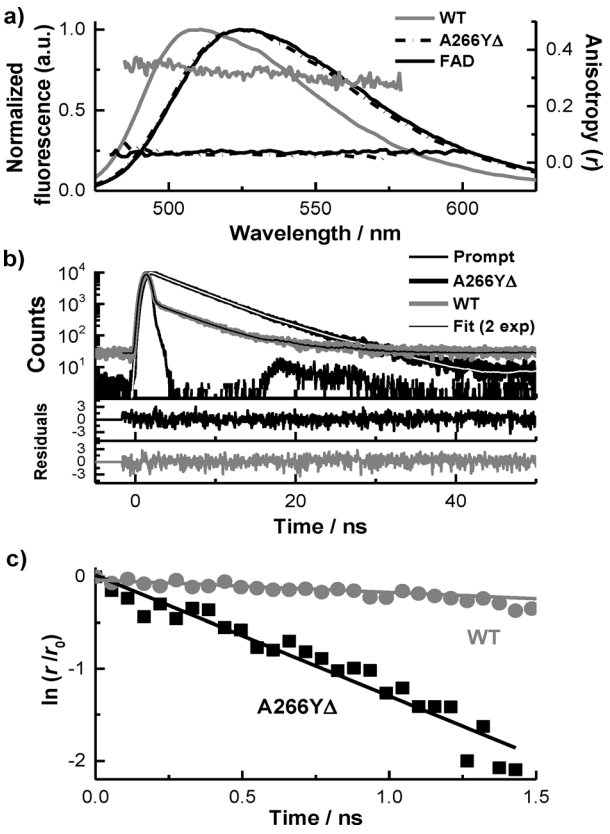

Figure 4. a) Normalized fluorescence emission spectra of WT and A266YΔ *Rc*FPR and FAD in air-saturated Tris buffer (50 mM, pH 8), with excitation at 450 nm, together with the respective emission anisotropy *r*. b) Fluorescence emission decay of WT and A266YΔ *Rc*FPR obtained by NanoLED excitation at 460 nm and monitored at 510 and 540 nm, respectively, together with the fitting curves obtained by deconvolution using a two-exponential decay function. c) First-order fluorescence anisotropy decays of WT and A266YΔ *Rc*FPR.

For a better understanding of these results, the fluorescence dynamic behavior of the cofactor in all enzymes was also analyzed by TCSPC using excitation at 460 nm, as shown for both WT and A266YΔ enzymes (Figure 4b). The cofactor fluorescence decay in all *Rc*FPR enzymes was satisfactorily fitted using a two-exponential function (Table 3). For the WT, the short lifetime (≈65 ps) of the main decay component (≈95%) was complemented by a long-lived component of 4.52 ns (≈5%), yielding an average lifetime $\tau_F = 280$ ps. In contrast, the fluorescence decays of all modified *Rc*FPR enzymes were characterized by a main decay contribution (>96%) with an associated lifetime of ≈4.5 ns, and a minor contribution (≤4%) with lifetimes ranging between 1.5 and 2.1 ns, producing $\tau_F \approx 4.40$ ns (Table 3). Note that this dynamic behavior for FAD bound to the modified enzymes is similar to the single-exponential decay of flavin mononucleotide (FMN) in buffer solution ($\tau_F = 4.50$ ns), but completely dissimilar to that for free FAD in buffer, which was only satisfactorily fitted using a three-exponential function, yielding $\tau_F = 1.89$ ns (Table 3).

Table 3. Steady-state and dynamic fluorescence parameters of flavins and *Rc*FPR variants in-air-saturated Tris buffer (50 mM, pH 8).[a]

	λ_F [ns]	FWHM [nm]	Φ_F ($\times 10^2$)	r[b]	τ_1 [ns] (% f_1)	τ_2 [ns] (% f_2)	τ_3 [ns] (% f_3)	τ_F [ns]	χ^2	θ_c [ns]
WT	511	68	1.6	0.323	0.07 (95)	4.52 (5)	–	0.29	1.083	7.45
A266Δ	523	74	35	0.030	1.53 (4)	4.52 (96)	–	4.39	1.127	0.78
A266YΔ	524	74	30	0.026	1.87 (3)	4.51 (97)	–	4.44	1.071	0.82
A266Y	523	75	23	0.032	2.07 (3)	4.56 (97)	–	4.47	1.042	0.79
FAD	526	76	28	0.023	0.22 (42)	2.23 (36)	4.52 (22)	1.89	1.091	0.89
FMN	523	76	220	0.010	4.50 (100)	–	–	4.50	1.101	0.75

[a] Experimental error ≤5%. [b] Value at the emission maximum.

The decay-associated spectra (DAS) of FAD in WT and modified enzymes were obtained by global fitting analysis of the fluorescence decays between 480 and 650 nm (Figure 5). In the case of WT, the ultrafast decay (65 ps) mainly corresponds to a blue-shifted emission of FAD with $\lambda_F^{max} = 508$ nm, and a minor contribution (5%) of red-shifted emission with $\lambda_F^{max} = 525$ nm and associated lifetime of 4.52 ns. Conversely, the DAS of modified enzymes showed two spectral contributions of FAD with a similar band maximum $\lambda_F^{max} \approx 525$ nm, but with associated lifetimes of 1.50 and 4.45 ns for the minor and major (>96%) components, respectively. Therefore, the DAS of the *Rc*FPR enzymes confirms the nanoscale environmental differences in the FAD-binding site between WT and its variants.

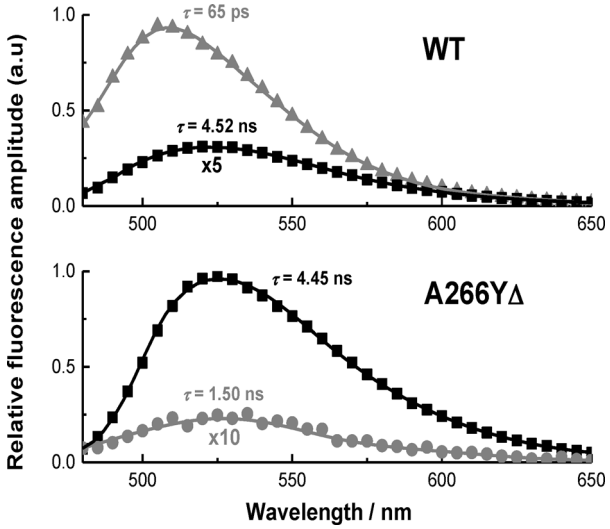

Figure 5. Decay-associated spectrum (DAS) of FAD obtained by global fit analysis of the fluorescence decay signals of WT and A266YΔ *Rc*FPR.

In addition, the anisotropy fluorescence decay of FAD bound to WT and modified enzymes yielded rotational correlation time $\theta_c = 7.4 \pm 1.5$ and $\approx 0.8 \pm 0.5$ ns, respectively, by assuming a depolarization mechanism of a spherical rotor decaying according to a first-order law (Figure 4c and Table 3). The θ_c values for modified *Rc*FPR enzymes were similar to that for free FAD. Therefore, both dynamic and steady-state anisotropy results indicate that a large impediment to the segmental motion of the isoalloxazine ring of the cofactor is produced only in WT *Rc*FPR.

Finally, by comparing the average fluorescence parameters of the modified and native enzymes (Table 3), that is, $\Phi_F^{Mutant}/\Phi_F^{WT} \approx \tau_F^{Mutant}/\tau_F^{WT} \approx 17 \pm 2$, it can be supposed that C-terminal manipulation produces a large decrease of the intraprotein quenching efficiency of the isoalloxazine ring in the WT enzyme.[14] However, although the FAD fluorescence in the modified *Rc*FPR enzymes behaves dynamically similar to FMN in buffer, which can be considered as an unquenched isoalloxazine ring model, the comparison of their fluorescence parameters yields $\Phi_F^{FMN}/\Phi_F^{Mutant} \gg \tau_F^{Mutant}/\tau_F^{WT} \approx 1$, suggesting the existence of a static fluorescence quenching effect of FAD by the surrounding amino acids in the modified enzymes.

2.4. Photosensitizing Properties of Modified Enzymes

The triplet excited state of fully oxidized flavins has been well characterized using transient absorption spectroscopy,[15] and because the ground state of fully oxidized FAD is spectroscopically transparent at >500 nm, the transient difference absorption spectra at the orange-red spectral region (550–750 nm) is only a measure of the formation and decay of the triplet excited state of the flavin, with a typical absorption maximum at approximately 715 nm.[4,15] Figure 6a shows the transient absorption decays of ^{3}FAD* monitored at 710 nm after laser excitation at 355 nm for A266Δ, and for the free flavin in air-saturated buffer solutions under identical experimental conditions. To avoid photodegradation of the samples, up to five single laser shots were averaged. Despite the weak transient absorption, in both cases the ^{3}FAD* transient signals were reasonably fitted as single-exponential decays, yielding similar lifetimes, for example, $\tau_T^{Air} \approx 2.5 \pm 0.3$ μs. In contrast, transient absorption experiments with WT *Rc*FPR under the same experimental conditions did not show any measurable transient signal attributable to ^{3}FAD*. Also, transient absorption decays obtained in argon-saturated buffer solutions of the free FAD and A266Δ *Rc*FPR yielded triplet lifetimes τ_T^{Air} of approximately 11 and 5 μs, respectively. As flavins are efficiently quenched by several electron-donor amino acids,[16] a lower τ_T^{Air} value for ^{3}FAD* in the modified enzymes could be expected, due to intraprotein quenching by the enzyme milieu.

Knowledge of the triplet lifetimes obtained in argon- and air-saturated solutions allowed the estimation of the apparent

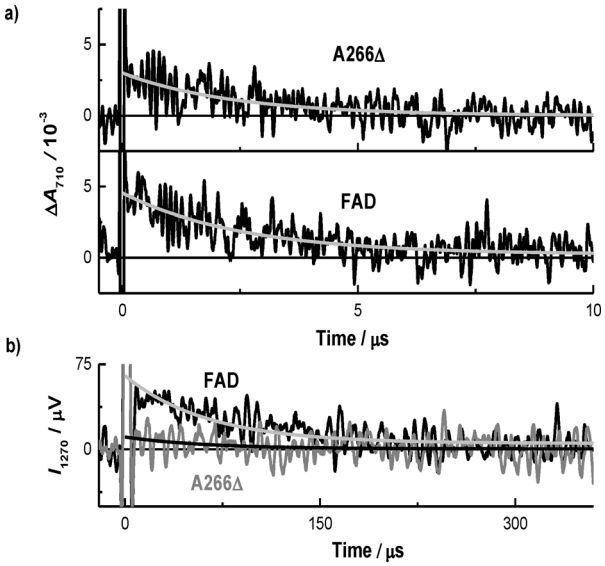

Figure 6. a) Transient absorption decay of the triplet excited state of FAD, monitored at 710 nm, obtained by ns-laser flash photolysis with laser excitation at 355 nm of free FAD and A266Δ *Rc*FPR in air-saturated Tris buffer (50 mM, pH 8). b) $^1O_2$ phosphorescence decay signal monitored at 1270 nm after photosensitization of free FAD and A266Δ *Rc*FPR in air-saturated deuterated solutions. All solutions were matched in absorbance at the excitation wavelength, for example, $A_{355} = 0.4$ ([FAD] ≈ 40 μM) and up to five single laser shots were averaged to avoid sample photodegradation. The transient signals were fitted as first-order kinetics.

quenching rate constant of the flavin triplet by $^3O_2$, $k_q^{O_2}$, in air-saturated solutions in which $[O_2]_{Air} = 0.27$ mM [Eq. (1)]:

$$k_q^{O_2} = \frac{(\tau_{T,Air})^{-1} - (\tau_{T,Ar})^{-1}}{[O_2]_{Air}} \quad (1)$$

The calculated $k_q^{O_2}$ values were $1.1 \pm 0.1 \times 10^9\ M^{-1}s^{-1}$ and $7.4 \pm 0.2 \times 10^8\ M^{-1}s^{-1}$ for free FAD and A266Δ *Rc*FPR, respectively. Assuming a homogeneous distribution of dissolved molecular oxygen in the buffer, the lower $k_q^{O_2}$ value obtained for the modified enzyme could indicate that the accessibility of $^3O_2$ to the cofactor triplet state is partially hindered in the binding site, as recently reported for the quenching of the triplet excited state of the dye Rose Bengal bound within human[17] and bovine serum albumin.[18]

By comparison of the extrapolated initial triplet absorbance difference (ΔA_0) values observed under both argon- and air-saturated solutions of free FAD and A266Δ *Rc*FPR, a triplet quantum yield of $\Phi_T^{mutant} = 0.10 \pm 0.03$ was estimated for the modified enzyme, assuming an identical molar absorption coefficient of the flavin triplet state in the enzyme than in buffer solution, and $\Phi_T = 0.15$ for FAD in aqueous media.[19]

The quenching of free ^{3}FAD* by dissolved $^3O_2$ generates singlet molecular oxygen ($^1O_2$) with relatively low quantum yield, for example, $\Phi_\Delta = 0.07$, as compared with other flavins such as FMN and riboflavin ($\Phi_\Delta \approx 0.50$).[20] The phosphorescence transient signal of $^1O_2$ observed after pulsed laser photosensitization of free FAD in air-saturated deuterium oxide (D_2O) solutions is shown in Figure 6b. This signal decays with a lifetime of $\tau_\Delta = 63 \pm 4$ μs, an expected value for this media.[21] In contrast, laser excitation of A266Δ *Rc*FPR under identical conditions produces a weak transient phosphorescence signal, closer to the detection limit of our experimental set-up (Figure 6b). Due to the poor signal-to-noise ratio of the $^1O_2$ phosphorescence decay generated by A266Δ, to obtain a reliable upper limit of the initial phosphorescence intensity (I_0) value, which is proportional to Φ_Δ, the decay portion of the signal was fitted exponentially using, as a fixed parameter, the $^1O_2$ lifetime obtained by photosensitization with FAD in buffer, for example, $\tau_\Delta = 63$ μs. Thus, a relative initial phosphorescence intensity value of $I_0^{FAD} \approx 7 \times I_0^{A266\Delta}$ was obtained.

In order to confirm the photosensitized generation of $^1O_2$ by the modified *Rc*FPR enzymes, steady-state photolysis experiments were also performed to measure the initial rate of $^3O_2$ uptake ($\nu_0^{O_2}$) due to the reaction between $^1O_2$ and added Trp (140 μM), which proceeds with a rate constant of $3 \times 10^7\ M^{-1}s^{-1}$,[22] yielding oxidation products with a characteristic excitation and emission fluorescence fingerprint.[23]

Figure 7a shows a comparison of the $^3O_2$-uptake kinetic curves obtained using 40 μM free FAD, and WT and A266Δ *Rc*FPR enzymes as photosensitizers in sealed air-saturated buffer solutions. As blue-light photolysis conditions were constant in all cases, the relative values of $\nu_0^{O_2}$ (i.e. the initial slopes in Figure 7a) can be also considered as a relative measurement of Φ_Δ. In the present case, $(\nu_0^{O_2})_{FAD+Trp} \approx 8 \times (\nu_0^{O_2})_{A266\Delta+Trp}$ was found, whereas for WT *Rc*FPR practically no $^3O_2$ uptake by added Trp was produced, which is in agreement with the lack

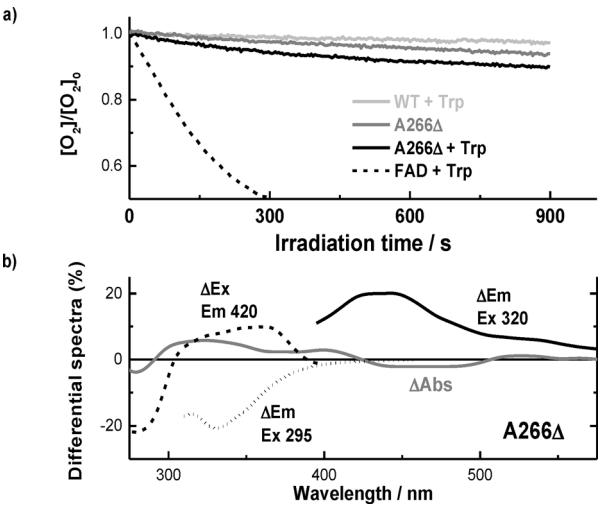

Figure 7. a) O_2-uptake profiles produced by steady-state photolysis at 462 ± 27 nm of FAD (40 μM) or native and A266Δ *Rc*FPR in air-saturated buffer with the addition of Trp (140 μM), and for A266Δ alone. b) Differential UV/Vis absorption and fluorescence excitation and emission spectral after 900 s of photosensitization of A266Δ *Rc*FPR (40 μM) with the addition of Trp (140 μM).

of triplet flavin transient absorption observed previously. Interestingly, photosensitization of A266Δ alone also shows a smaller $\nu_0^{O_2}$, for example, $(\nu_0^{O_2})_{A266\Delta} \approx 0.2 \times (\nu_0^{O_2})_{A266\Delta+Trp}$. This minor $^3O_2$ uptake can be due to self-oxidation of amino acid residues of the enzyme backbone, such as the more solvent-exposed Trp residues, as suggested by the differential UV/Vis and fluorescence spectral changes observed after 900 s of blue-light photolysis (Figure 7b). A decrease in the emission band of Trp, selectively excited at 295 nm, was observed, together with the formation of a new fluorescence band centered on 450 nm that corresponds to an excitation spectrum between 310–380 nm. Similar spectral changes were observed also for the FAD and A266Δ solutions containing added Trp. However, after photolysis of the WT enzyme in presence of Trp, no spectral changes were observed. Thus, considering both sets of photosensitization experiments and $\Phi_\Delta^{FAD} = 0.07$,[20] the comparison of either I_0 or $\nu_0^{O_2}$ values obtained for the modified enzyme and free FAD, the maximum value of quantum yield of $^1O_2$ formation, $\Phi_\Delta = 0.010 \pm 0.004$, was estimated for A266Δ *Rc*FPR.

3. Discussion

3.1. Specific Interaction between FAD and Tyr66 Prevents WT *Rc*FPR Photodegradation

The results described above indicate that the site-specific mutation and/or scission of the terminating peptide FVGEGI of the mobile C-terminal extension of *Rc*FPR impact on both the spectroscopic and photophysical properties of the cofactor FAD, in addition to the reported decrease of enzymatic activity.[2b]

A remarkable result is that WT *Rc*FPR does not show any photochemical degradation process in contrast with the C-ter-

minal modified enzymes. As the isoalloxazine ring of the bound FAD molecule is fully oxidized, absorption of both UVA and blue light to populate the singlet excited state of FAD (^{1}FAD*) occurs, and hence to block any route to photochemical degradation in the WT enzyme, an efficient quenching mechanism of ^{1}FAD* must be operative.

One plausible quenching mechanism of ^{1}FAD* in the native enzyme could be the ultrafast intramolecular electron-transfer (ET) process from the adenine moiety to the isoalloxazine ring, produced by the stacking of both aromatic ring systems in a close co-planar configuration.[24] This intramolecular quenching mechanism operates in solution, in which transformation of "closed" (completely quenched) to "open" (unquenched) intramolecular conformers between the isoalloxazine and adenine rings is allowed.[24a] Thus, the three-exponential fluorescence decay of ^{1}FAD* observed in buffer, with average lifetime $\tau_F = 1.89$ ns (Table 3), is associated with the aforementioned molecular conformers. In fact, the observed τ_F value agrees well with the theoretical value (1.7 ns) obtained by molecular dynamic modeling of the conformation dynamics in water,[24a] reflecting a similar average conformational distribution of FAD independently of the presence of Tris buffer. The crystal structures of WT (PDB ID: 2BGJ) and A266YΔ (4K1X) enzymes indicated that FAD is bound in a partially extended conformation, with the ribityl-pyrophosphate-ribofuranosyl chain fixed by hydrogen-bond interactions with several amino acids belonging to the FAD-binding domain, and with the isoalloxazine and adenine moieties separated at a distance of approximately 3.3 Å.[2b] This short distance could be appropriate for efficient π–π interactions, however both rings are intercalated by the peptide chain and orientated almost perpendicularly (Figure 8a),[2b] avoiding the possibility of co-planar stacking between the donor–acceptor aromatic rings as occurs in fluid solutions. Therefore, the deactivation of ^{1}FAD* by adenine cannot be expected to occur in both WT and modified *Rc*FPR enzymes.

In this case, the efficient deactivation of ^{1}FAD* observed in WT *Rc*FPR must be ascribed to specific interaction(s) between the isoalloxazine fluorophore and close amino acid residue(s) that can act as efficient charge-transfer (CT) quenchers.[25] The occurrence of such an efficient quenching mechanism is evidenced by the almost 17-fold increase of both fluorescence quantum yield Φ_F and average fluorescence lifetime τ_F in the modified enzymes as compared with the WT (Table 3), confirming that the C-terminal manipulation abates the intraprotein deactivation of ^{1}FAD*. It has been demonstrated in femtosecond emission spectroscopy studies of several "nonfluorescent" or weakly fluorescence flavoenzymes, such as riboflavin-binding protein (RBP) and glucose oxidase (GOx) that a prompt (< 10 ps) CT quenching of the flavin from the aromatic residues is produced.[6,26] The common feature of these flavoproteins is that they contain Tyr and/or Trp residues in close proximity to the isoalloxazine ring of the flavin cofactor, for example, less than 5 Å, and are oriented appropriately for ultrafast ET from the aromatic amino acid to the flavin. In the particular case of Tyr, the ET process is followed by a proton-transfer (PT) reaction involving the OH group of the amino acid.[6,26]

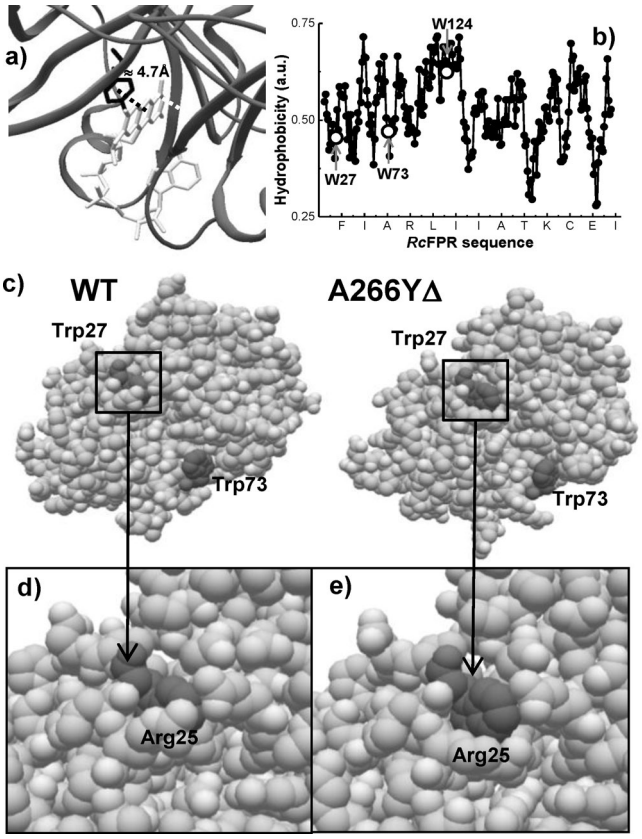

Figure 8. a) Tyr66 distance (≈4.7 Å) and conformation from the *face* side of the isoalloxazine ring of FAD in WT *Rc*FPR (PDB ID: 2BGJ). b) Hydrophobicity for amino acid residues of *Rc*FPR enzymes as calculated using ProtScale (ExPASy Bioinformatics Resource Portal).[29] c) Representation of edge exposed to the bulk solvent of residues Trp27 and Trp73 present in WT (2BGJ) and A266YΔ (4K1X) *Rc*FPR enzymes. Zoom of conformational differences around Trp27 in WT (d) and A266YΔ (e), in which the displacement of Arg25 in A266YΔ suggests higher accessibility and/or interaction with solvent molecules for this Trp residue.

Thus, the close spatial proximity between the cofactor and the electron/proton donors favors a barrierless and/or coherent process coupled with the appropriate vibrational modes of the isoalloxazine and intraprotein environment. As well as the lower resolution limit of our TCSPC system (≈55 ps), the measured fast component in the fluorescence decay at 510 nm of WT *Rc*FPR of approximately 65 ps is associated with the prompt CT quenching of the singlet excited state of the isoalloxazine fluorophore by a close aromatic amino acid. In accordance with the crystallographic structure of WT *Rc*FPR (Figure 8a), only the highly conserved residue Tyr66 is located within approximately 4.7 Å in an almost co-planar orientation from the isoalloxazine ring of FAD.[2b] In this case, this residue can be responsible for the larger absorbance ratio (A_{480}/A_{450}) observed for the WT enzyme (Table 1); substitution of the Tyr residue located very close to the isoalloxazine ring in native flavoenzymes for Ala or Phe decreases the intensity of the red-shifted vibronic shoulder.[9,10] In fact, scission of the ending peptide, Δ = FVGEGI, lowers the A_{480}/A_{450} ratio (Table 1), suggesting that the loss of this C-terminal hexapeptide decreases the specific interaction of the isoalloxazine ring with Tyr66.

Surprisingly, the insertion of an extra Tyr residue in the NADP(H)-binding domain of both A266Y and A266YΔ enzymes yielded intermediate values of A_{480}/A_{450} (Table 1). As is discussed below, this result suggests that specific interactions with the isoalloxazine ring are not increased by the addition of Tyr residues at position 266.

Therefore, if the Tyr66 residue is the only amino acid located in an appropriate distance from, and orientation with, the isoalloxazine ring to produce the prompt deactivation of ^{1}FAD* in WT *Rc*FPR, the most probable self-photoprotection mechanism of the native enzyme is given by the following coupled ET and PT process, as proposed by Mataga et al.[6,26] [Eqs. (2–5)], by which the absorbed photons are promptly (< few ps) converted into heat energy, thus avoiding any harmful secondary processes:

$$(\mathrm{FAD}\cdots\mathrm{Y66\text{-}OH})_{WT} \xrightarrow{h\nu} (\mathrm{FAD}^*\cdots\mathrm{Y66\text{-}OH})_{WT} \quad (2)$$

$$(\mathrm{FAD}^*\cdots\mathrm{Y66\text{-}OH})_{WT} \xrightarrow{k_{ET}} (\mathrm{FAD}^{\bullet-}\cdots\mathrm{Y66\text{-}OH}^{\bullet+})_{WT} \quad (3)$$

$$(\mathrm{FAD}^{\bullet-}\cdots\mathrm{Y66\text{-}OH}^{\bullet+})_{WT} \xrightarrow{k_{PT}} (\mathrm{FADH}^{\bullet}\cdots\mathrm{Y66\text{-}O}^{\bullet})_{WT} \quad (4)$$

$$(\mathrm{FAD}^{\bullet}\cdots\mathrm{Y66\text{-}O}^{\bullet})_{WT} \xrightarrow{k_{back}} (\mathrm{FAD}^*\cdots\mathrm{Y66\text{-}OH})_{WT} \quad (5)$$

3.2. C-terminal Modification Induces Subtle Global Conformational Changes

Shifts in intrinsic Trp fluorescence bands are commonly used to monitor structural changes in proteins and to make inferences regarding local structure and dynamics.[12,27] The intrinsic maximum emission of WT *Rc*FPR at 323 nm corresponds to the typical emission of a buried or hydrophobic Trp residue, and termed class 1.[12b] In accordance with the reported 3D PDB structure of both WT and A266YΔ enzymes,[2b] of the three Trp residues present, only Trp124 is completely buried in the protein chain, whereas both Trp27 and Trp73 are edge-exposed to the bulk solvent (Figure 1). The hydrophobic nature of Trp124 was also confirmed by analysis of the hydrophobicity of the native enzyme as developed by Black and Mould[28] and analyzed with the free software Protscale[29] (Figure 8b). This residue is located in the sequential region with highest hydrophobicity of the enzyme, whereas both Trp27 and Trp73 residues are in regions with lower degree of hydrophobicity. Therefore, the blue-shifted intrinsic fluorescence of WT *Rc*FPR can be mainly assigned to the emission of the buried Trp124.

The C-terminal modification of the WT enzyme produces a moderate redshift of the intrinsic emission band, together with a slight increase of both Φ_F and τ_F; these are larger for enzymes lacking the ending peptide Δ = FVGEGI, that is, A266YΔ and A266Δ (Table 2). This behavior reflects a modest change in the nano-environment around the Trp residues upon C-terminal manipulation, becoming to a certain degree polar but not completely exposed to water molecules, as reported for edge-exposed Trp residues (class 2).[12b] However, despite the more hydrophobic and rigid nano-environment sensed by the Trp residues in the *Rc*FPR variants, the lower Φ_F and τ_F values observed for the enzymes than for free Trp in buffer solution (Table 2) suggest the occurrence of intraprotein quenching effects on the Trp residues, as an increase in Φ_F and τ_F should be expected for indole derivatives in more hydrophobic and/or rigid media.[12a,30] Figure 8c–e shows a comparison of the spatial positions of the Trp residues and their environments using crystallographic data for the WT (PDB ID: 2BGJ) and A266YΔ (4K1X), confirming that after enzyme modification, Trp27 shows a small displacement of about 0.6–0.8 Å over the same plane, together with a displacement of the surrounding Arg25 relative to the positions in the WT enzyme. Although Trp73 shows no changes in its immediate neighbors (only Glu75 appears oriented differently), the α-helix from Leu173 to Lys186 in A266YΔ is closer compared to that of WT.[2b] Finally, for the highly hydrophobic Trp124, neither spatial nor surrounding environment changes were noticed. Thus, it can be expected that C-terminal modification of the enzyme produces subtle structural changes in the protein backbone that slightly affect the intrinsic fluorescence of the most external Trp residues—Trp27 and Trp73—probably by a complex combined effect of solvent (water) and intrinsic protein interactions.[12b]

The average steady-state anisotropy *r* associated with the intrinsic Trp fluorescence of all *Rc*FPR variants was around 0.220 ± 0.010 (Table 2). This value is threefold larger than that of free Trp in the same buffer solution and closer to the fundamental anisotropy of Trp ($r_0 \approx 0.280$, excitation at 295 nm[31]), which is the maximum anisotropy value that can be expected in the absence of other depolarizing processes such as rotational diffusion or energy transfer. Thus, using both average *r* and τ_F values for the *Rc*FPR enzymes calculated from the data shown in Table 2 in the modified Perrin equation [Eq. (6)], which contains the empirical factor 2 for taking into account the effect of the solvent hydration shell of the protein,[12a,32] a rotational correlation time $\theta_c^{RcFPR} = 18 \pm 3$ ns was estimated for the enzymes:

$$\theta_c^{RcFPR} \approx 2\tau_F^{RcFPR}\left(\frac{r_0^{Trp}}{r^{RcFPR}} - 1\right)^{-1} \quad (6)$$

The calculated θ_c^{RcFPR} value agrees well with that expected for proteins of around 30 kDa;[12a,32] the present case is 33 kDa. Therefore, it can be concluded that segmented rotation of the emitting Trp residues in the *Rc*FPR variants is almost completely hindered and the fluorescence depolarization is mainly produced by the slower "tumbling" of the whole enzyme.

3.3. The C-Terminal Peptide FVGEGI Controls the Photophysics of FAD

The larger blue-shift and narrower band of the cofactor fluorescence emission indicates that the isoalloxazine ring of FAD in WT *Rc*FPR (Figure 4a) senses a much less polar environment than in the modified proteins and in bulk aqueous buffer.[4,15b] Furthermore, both steady-state and dynamic anisotropy data for WT *Rc*FPR are single-fold larger than for the modified enzymes (Table 3), confirming that the isoalloxazine ring of FAD in the WT enzyme is more deeply buried than in the modified

enzymes. This local rigidity of the isoalloxazine ring in the WT enzyme seems to be a key factor in maintaining its interaction with the Tyr66 residue, and hence induces an efficient quenching effect of ^{1}FAD* as discussed before.

The rotational correlation time $\theta_c = 7.4$ ns, obtained from time-resolved anisotropy measurements for bound FAD in WT enzyme (Figure 4c), was shorter than that calculated with Equation (6) using the intrinsic Trp fluorescence of the enzymes, as discussed above. This discrepancy can be consequence of a more efficient depolarization of the excited flavin by the ultrafast CT quenching process involving Tyr66 [Eqs. (2–5)]. In turn, the steady-state anisotropy of the *Rc*FPR enzymes slightly decreased with the monitoring wavelength, especially for WT (Figure 4a). As the dynamic Stokes shift of the excited Frank–Condon (FC) of flavins enclosed by protein can be considered an ultrafast process (<100 fs),[6,26] the anisotropy decrease with emission wavelength could be associated with the existence of different enzyme conformers or substates, as previously evidenced by crystallographic analysis of these enzymes.[2b] The analysis of the DAS (Figure 5) supports the notion that for WT the main ultra-short fluorescence component of 65 ps corresponds to a conformational population of the enzyme in which FAD senses a highly hydrophobic and rigid nano-environment, a prerequisite for efficient quenching by the closer Tyr66 residue. Only <5% of WT enzyme population presents a conformation with the isoalloxazine ring located in a more polar and fluid nano-environment, and thus the FAD emission properties of this conformer, such as lifetime and anisotropy, resemble those observed for FMN in aqueous solution. Therefore, for bound FAD conformers the depolarized red-shifted emission ($\lambda_F^{max} = 525$ nm) with an associated lifetime of approximately 4.5 ns should indicate the lack of interactions with surrounding aromatic amino acids, such as Tyr66.

This should also be the case for all the *Rc*FPR variants, as both the lack of anisotropy and the red-shifted emission of the DAS components indicate that the isoalloxazine ring of bound FAD in the mutants is not interacting with Tyr66, as occurs with the WT enzyme. However, despite the larger mobility and solvent exposure of the isoalloxazine ring of FAD in the modified enzymes, a minor fraction of conformers (<4%) showed a shorter associated lifetime of approximately 1.5 ns, indicating quenching effects by the surrounding amino acids.

At this point, it is worth noting the fluorescence behavior of FAD in A266Y and A266YΔ enzymes, which contain the extra Tyr266 residue. As already mentioned, the reported 3D crystal structure of A266YΔ suggested the existence of two asymmetric units of the enzyme, one with the phenol moiety of Tyr266 in close stacking with the *re* face of the isoalloxazine ring,[2b] resulting in a "sandwich" conformation together with the conserved Tyr66 from the other face, as found in plant FNR enzymes.[1b] Conversely, in the other conformer, the phenol group of Tyr266 points toward the adenine moiety of FAD, in the opposite direction to the isoalloxazine ring.[2b] In accordance with the ultrafast CT quenching mechanism of the excited singlet state of flavins by nearby aromatic amino acid residues,[6,26] for a "sandwich" conformation, as in the case of both A266Y and A266YΔ, an even more efficient CT-quenching effect should be expected than for WT *Rc*FPR. However, the fluorescence enhancement observed for both modified enzymes indicates that this is not the case, and therefore it can be concluded that the isoalloxazine ring is almost not interacting with either Tyr66 or Tyr266, and therefore the major conformer in solution is that in which the phenol group of Tyr266 is located away from the isoalloxazine ring.

3.4. Photosensitizing Properties of C-Terminal Modified *Rc*FPR Enzymes

The changes in the specific interactions between the isoalloxazine moiety of FAD and the surrounding amino acids by alteration of the C-terminal tail of the WT *Rc*FPR induce the population of both singlet and triplet excited states of the cofactor. Both the triplet quantum yield and lifetime of FAD for the modified enzymes in argon-saturated solutions were lower than those observed for FAD in water, indicating that the enzyme environment also induces the prompt quenching of ^{3}FAD*.[4,16]

In contrast, in air-saturated solutions of modified enzymes, the bound ^{3}FAD* is quenched by dissolved O_2 with less efficiency than free ^{3}FAD* in buffer, suggesting that the FAD-binding domain preclude the free diffusion of dissolved $^3O_2$, as it was also found for the $^3O_2$-quenching of the triplet excited state of the dye Rose Bengal bound within the hydrophobic Sudlow's site I of either human[17] or bovine serum albumin.[18]

Nevertheless, the $k_q^{O_2}$ value for the $^3O_2$-quenching of ^{3}FAD* in the modified enzymes is almost one-order of magnitude lower than the diffusional controlled limit in water, that is, $k_{diff} \approx 6\times10^9\ M^{-1}s^{-1}$, as typically expected for $^3O_2$-mediated quenching processes of excited triplets governed by energy-transfer pathway to generate singlet molecular oxygen $^1O_2$:[33]

$$(^3\mathrm{FAD}^*)_{mutant} + {}^3O_2 \xrightarrow{k_q^{O_2}} (\mathrm{FAD})_{mutant} + {}^1O_2 \qquad (7)$$

The generation of $^1O_2$ by the quenching process described by Equation (7) in the modified enzymes occurred with low quantum yield, for example, $\Phi_\Delta \approx 0.010$, as determined by both direct $^1O_2$-phosphorescence decay detection and $^3O_2$ uptake in the presence of Trp (Figures 6b and 7a). The agreement between both methods suggests that $^1O_2$ is the main reactive oxygen species (ROS) produced by photosensitization of the *Rc*FPR variant. The estimated Φ_Δ value for the modified *Rc*FPR is closer to that reported for the FMN-bearing flavoprotein called miniSOG (i.e. mini "singlet oxygen generator", with $\Phi_\Delta = 0.03 \pm 0.02$),[7,34] a fusion protein derived from *Arabidopsis thaliana* phototropin 2, in which, among other changes, a cysteine residue positioned near the bound FMN was replaced with a Gly residue (C426G).[35] It is interesting to compare both modified flavoproteins, as a higher Φ_Δ value could be expected for miniSOG considering the higher intrinsic Φ_Δ value of FMN (≈ 0.50) compared with FAD (≈ 0.07). However, miniSOG displayed an almost 20-fold decreases of Φ_Δ compared with free FMN—a consequence of an enhanced ET-based or type I mechanism production of oxygen radicals, for example, anion superoxide $O_2^{\bullet-}$, as the main source of photosensitized ROS.[7]

Conversely, the decreases of Φ_Δ in modified *Rc*FPR as compared with free FAD can be assigned mainly to the prompt quenching of ^{3}FAD* by the enzyme milieu, as the experimentally determined ratio $\Phi_\Delta^{mutant}/\Phi_\Delta^{FAD} = 0.14 \pm 0.04$ is almost the same value as that of the efficiency of ^{3}FAD* quenching by the enzyme, $^3\eta_q$, as calculated with Equation (8), in which the first and second terms represent the static and dynamic quenching efficiencies of ^{3}FAD*, respectively:

$$^3\eta_q = \left(1 - \frac{\Phi_T^{mutant}}{\Phi_T^{FAD}}\right)\left(1 - \frac{\tau_{T,Argon}^{mutant}}{\tau_{T,Argon}^{FAD}}\right) = 0.18 \pm 0.03 \quad (8)$$

Therefore, a comparison of the photophysical and photosensitizing properties of the two flavoproteins miniSOG and modified *Rc*FPR suggests that a rather complex interplay between the flavin cofactor (i.e. FMN or FAD) and the surrounding amino acid environment in the binding cavity controls the photophysical and photochemical fate of the flavin.

The $^1O_2$-mediated oxidation of intrinsic Trp residues in the enzyme, and also of extrinsic Trp added as a $^1O_2$ trap by blue-light photosensitization of A266Δ, was confirmed by the fluorescence spectral changes under different excitation and emission monitoring conditions (Figure 7). The differential fluorescence spectra after 900 s of photolysis indicated that the decrease of the emission band of Trp between 300–450 nm, obtained by excitation at 295 nm, was accompanied with the growth of new excitation and emission bands between 300–400 nm and 400–550 nm, respectively. These new fluorescence bands are associated with the formation of $^1O_2$-mediated oxidized products of Trp, such as kynurenine and/or indole like derivatives.[23,36] Indeed, the differential UV/Vis absorption spectra also indicates the degradation of chromophores absorbing at 280 nm, as expected for Trp consumption, and the formation of new chromophores that absorb at 300–400 nm, corresponding to the formation of Trp-oxidation products.[23] Nevertheless, the $^1O_2$-mediated oxidation of other amino acids such as Met and His cannot be overlooked,[36] as their respective oxidation products are almost undetectable by either absorption or emission spectroscopies. The slight bleaching of the visible band of FAD observed after photolysis of the enzyme suggests the occurrence of a minor CT degradation channel of the flavin.

Finally, although not trivial, the photolysis of the WT enzyme solution did not produce any absorbance and fluorescence spectral changes (data not shown), confirming its photochemical inactivity, a relevant prerequisite for the preservation of the enzyme stability and functionality.

4. Conclusions

In this study, we have demonstrated, by using absorption and emission spectroscopies, that deletion of the C-terminal hexapeptide FVGEGI beyond Ala266, combined with the site-specific mutation A266Y in *Rc*FPR introduces structural and conformational changes to the cofactor-binding site. This not only strongly reduces its catalytic activity, as we have previously reported,[2b] but that also enhances both the photophysical and photochemical properties of the bound cofactor.

Either the specific A266Y mutation or peptide deletion, or their combination, result in the distortion and decrease in rigidity of the FAD-binding domain, altering the appropriate distance between and orientation of the isoalloxazine ring with Tyr66, a nearby and highly conserved residue, avoiding the efficient ultrafast CT quenching of ^{1}FAD* by this aromatic amino acid residue. As a result, the photophysical properties of bound FAD in the modified enzymes are enhanced, for example, fluorescence quantum yield and lifetimes increase, and also allow population of the long-lived ^{3}FAD*. Under aerobic conditions, in turn, dissolved $^3O_2$ is able to quench ^{3}FAD* producing singlet molecular oxygen $^1O_2$ with a quantum yield of $\Phi_\Delta \approx 0.01$, which is the main ROS responsible for the oxidation of intrinsic and extrinsic molecular targets, such as Trp.

Therefore, the results of this study reflect the delicate balance between conformation and functionality of flavoproteins, and as a result of their genetic manipulation; in the case of WT *Rc*FPR, the conformational arrangement of the C-terminal motif is associated with both efficient enzymatic activity and protective mechanism against self-photodegradation processes.

Experimental Section

Materials

All chemicals were analytical purity grade products of Sigma–Aldrich, and were used as received. All solutions were prepared using deionized water (Milli-Q, Millipore).

Enzyme Handling and Activity

The vectors used for enzyme expression were designed according to Bortolloti et al.[2b] In brief, fused proteins (thioredoxin–His_6) were expressed after transformation of competent *Escherichia coli* BL21(DE3)pLysS cells and induction with isopropyl β-D-1-thiogalactopyranoside, (0.5 mM) at 20 °C for 16 h. Cell lysates were purified by metal-affinity chromatography (Ni–NTA, Qiagen) and dialyzed against Tris buffer (50 mM, pH 8). Proteins were further digested with enterokinase to release the hexahistidine tag and purified using Q-sepharose chromatography. All fractions were analyzed using sodium dodecyl sulfate–polyacrylamide gel electrophoresis (SDS-PAGE), with Coomassie Brilliant Blue staining. The molecular weight of WT *Rc*FPR is 33 kDa.

Diaphorase activity was confirmed in situ, using native PAGE, with non-denaturing buffer (Laemmli without SDS).[37] Activity staining was carried out by incubation in Tris-HCl (50 mM, pH 8.0) containing $NADP^+$ (0.3 mM), glucose-6-phosphate (3 mM), glucose-6-phosphate dehydrogenase (1 unit mL^{-1}) and nitroblue tetrazolium (7.5 μg mL^{-1}). Activity bands were visualized by the formation of the violet formazan precipitate.[37] All purified enzymes showed similar diaphorase activity, as previously reported.[2b]

Prior to all measurements, solutions of purified enzymes in ice-cooled Tris buffer (50 mM, pH 8, 500 μL) were filtered through a Microamicon filter (cut-off 10 kDa) by centrifugation at 10 000 rpm with an Eppendorf mini-centrifuge (10 min, 4 °C). The proteins

were washed twice with the working buffer, and finally re-suspended in the same buffer to yield an absorbance at 450 nm ≈ 0.1.

All protein solutions were protected from ambient light to avoid photodegradation and in ice-cold baths, except during spectroscopic measurements, which were performed at 25.0 ± 0.1 °C. Finally, all spectroscopic and kinetic data are reported with their respective standard deviation representing the average values of three sets of experiments, with independent purification of each enzyme.

Steady-State UV/Vis Absorption and Fluorescence

UV/Vis absorption spectra were measured with an Agilent 8453 spectrophotometer (Palo Alto, CA). Fluorescence excitation and emission spectra were recorded with a Hitachi F-2500 spectrofluorimeter (Kyoto, Japan) equipped with an R-928 photomultiplier, in a 100 μL fluorescence quartz cell with an optical path length of 3 mm (Hellma, Müllheim, Germany). Emission spectra of the *Rc*FRP variants were obtained by excitation at 295 or 450 nm in order to excite selectively either the Trp residues or FAD, respectively. In all cases, 2.5 nm excitation slit was used and the emission slit was regulated between 2.5 and 10 nm, according to the fluorescence quantum yield of the sample, in order to obtain spectra with satisfactory signal-to-noise ratio. In addition, the excitation beam was attenuated with a neutral density filter with approximately 20% of transmittance to avoid photochemical processes during acquisition. The intrinsic and cofactor fluorescence quantum yields (Φ_F) of the enzymes in air-saturated buffer solutions were determined by comparison of the integrated fluorescence intensity using the emission spectra of authentic solutions of Trp ($\Phi_F^{Trp} = 0.14$)[12a] and FAD ($\Phi_F^{FAD} = 0.028$)[38] in the same buffer as reference, with matched absorbance ($A \approx 0.05$) at the excitation wavelength to minimize internal filter effects. The steady-state fluorescence anisotropy r of the samples was determined with a classical L-format and calculated as previously described.[38]

Time-Resolved Measurements

Fluorescence decays corresponding either to the intrinsic Trp or FAD emissions were obtained with a Tempro-01 TCSPC fluorimeter (Horiba, Glasgow, UK) using 1 Mhz pulsed LEDs (NanoLED, Horiba) emitting at 277 ± 11 or 461 ± 27 nm, for enzyme or cofactor excitation, respectively. Fluorescence detection was performed using a −30 °C cooled photomultiplier tube detector with < 10 dark counts (TBX-07C, Horiba) placed in the output of an f/4 emission monochromator calibrated at the emission maximum of the emitters with an output emission slit of 12 nm. A diluted Ludox scatter solution was used to register the instrumental response at the excitation wavelength and also to verify that no excitation scattered light was acquired at the emission wavelength. The fluorescence intensity and anisotropy decays were fitted with the fluorescence decay analysis software DAS6 (Horiba) by deconvolution of the pulse function using the multi-exponential model function.

Lifetime distributions were determined using the hybrid ME/NLS algorithm of the free software MemExp (version 4.0; NIH Center for Molecular Modeling, http://cmm.cit.nih.gov/memexp/) and the method fundamentals and working equations are reported elsewhere.[13]

Transient absorption signals of the excited triplet state of FAD (^{3}FAD*) in both air- and argon-saturated buffer solutions were recorded at 710 nm with the m-LFP 112 laser-flash photolysis system (Luzchem Research Inc., Ottawa, Canada) using the third harmonic from a Minilite II (Continuum Inc., Santa Clara, CA) Nd-YAG laser (355 nm, 7 ns full-width at half-maximum, FWHM, 5 mJ per pulse) as the excitation source.[15b]

Transient phosphorescence detection of singlet molecular oxygen ($^1O_2$) at 1270 nm, produced by 355 nm pulsed laser photosensitization of FAD in air-saturated deuterated (D_2O) solutions, to improve the phosphorescence detection of $^1O_2$, was performed with a Peltier-cooled Ge photodiode J16TE2-66G (Teledyne Judson Technology, Montgomeryville, PA). Under these experimental conditions, the lifetime of the decay portion of $^1O_2$ was much longer than the signal rise time, and therefore the transient phosphorescence signal was fitted to a first-order decay law.[39]

O_2-Uptake Measurements

The kinetics of O_2 uptake by blue-light photosensitization of FAD or enzyme solutions in the absence or presence of Trp (140 μM) as $^1O_2$-trap molecule were measured using a home-made system composed of a stainless-steel 1/16" FOXY-R-AF fiber-optic luminescent sensor system coupled with a CCD-USB2000 fluorimeter (OceanOptics, Dunedin, FL) placed on top of a sealed 5 × 5 mm path quartz cuvette (Hellma). The photosensitized consumption of dissolved oxygen was monitored for 900 s with continuous irradiation from a blue LED (462 ± 27 nm, 1 W) for excitation. Simultaneously, the absorption spectral changes of the solution were registered with an extra CCD-USB2000 spectrometer (OceanOptics), with the analyzing UV/Vis beam at right angle to the photolysis beam from the blue LED. Soft mixing of the enzyme solutions was done using a magnetic stirring bar to avoid foam formation. Excitation and emission spectra of the starting and final photolyzed solutions were also measured with the Hitachi F-2500 fluorimeter.

Acknowledgements

This research was supported by the Argentinean funding institutions Consejo Nacional de Investigaciones Científicas y Técnicas (CONICET, PIP 0374/12 and PIP 0365/11), Agencia de Promoción Científica y Tecnológica (ANPCyT, PICT 2012-2666), and Universidad Nacional de Santiago del Estero (UNSE-CICyT 23A/162). I.A., F.E.M.V., N.C, and C.D.B. are research members of CONICET.

Keywords: flavin triplet state · flavoproteins · fluorescence · oxidoreductases · singlet oxygen

[1] a) A. K. Arakaki, E. A. Ceccarelli, N. Carrillo, *FASEB J.* **1997**, *11*, 133 – 140; b) N. Carrillo, E. A. Ceccarelli, *Eur. J. Biochem.* **2003**, *270*, 1900 – 1915; c) E. A. Ceccarelli, A. K. Arakaki, N. Cortez, N. Carrillo, *Biochim. Biophys. Acta, Proteins Proteomics* **2004**, *1698*, 155 – 165; d) A. Aliverti, V. Pandini, A. Pennati, M. de Rosa, G. Zanetti, *Arch. Biochem. Biophys.* **2008**, *474*, 283 – 291.

[2] a) A. Bortolotti, I. Pérez-Dorado, G. Goñi, M. Medina, J. A. Hermoso, N. Carrillo, N. Cortez, *Biochim. Biophys. Acta, Proteins Proteomics* **2009**, *1794*, 199 – 210; b) A. Bortolotti, A. Sánchez-Azqueta, C. M. Maya, A. Velázquez-Campoy, J. A. Hermoso, M. Medina, N. Cortez, *Biochim. Biophys. Acta, Bioenergetics* **2014**, *1837*, 33 – 43.

[3] F. Mueller in *Chemistry and Biochemistry of Flavoenzymes, Vol. I* (Ed.: F. Mueller), CRC, Boca Raton, **1991**, pp. 1 – 71.

[4] P. F. Heelis, *Chem. Soc. Rev.* **1982**, *11*, 15 – 39.

[5] A. Möglich, X. Yang, R. A. Ayers, K. Moffat, *Ann. Rev. Plant Biol.* **2010**, *61*, 21 – 47.

[6] a) N. Mataga, H. Chosrowjan, S. Taniguchi, F. Tanaka, N. Kido, M. Kitamura, *J. Phys. Chem. B* **2002**, *106*, 8917 – 8920; b) N. Mataga, H. Chosrowjan, Y. Shibata, F. Tanaka, Y. Nishina, K. Shiga, *J. Phys. Chem. B* **2000**, *104*, 10667 – 10677.
[7] F. M. Pimenta, R. L. Jensen, T. Breitenbach, M. Etzerodt, P. R. Ogilby, *Photochem. Photobiol.* **2013**, *89*, 1116 – 1126.
[8] a) F. Mueller, S. G. Mayhew, V. Massey, *Biochemistry* **1973**, *12*, 4654 – 4662; b) J. K. Eweg, F. Mueller, A. Visser, C. Veeger, D. Bebelaar, J. D. W. Vanvoorst, *Photochem. Photobiol.* **1979**, *30*, 463 – 471; c) J. F. Cerda, R. L. Koder, B. R. Lichtenstein, C. M. Moser, A. F. Miller, P. L. Dutton, *Org. Biomol. Chem.* **2008**, *6*, 2204 – 2212; d) K. Yagi, N. Ohishi, K. Nishimoto, J. D. Choi, P. S. Song, *Biochemistry* **1980**, *19*, 1553 – 1557.
[9] A. Visser, P. A. W. van den Berg, N. V. Visser, A. van Hoek, H. A. van den Burg, D. Parsonage, A. Claiborne, *J. Phys. Chem. B* **1998**, *102*, 10431 – 10439.
[10] P. A. W. van den Berg, A. van Hoek, C. D. Walentas, R. N. Perham, A. Visser, *Biophys. J.* **1998**, *74*, 2046 – 2058.
[11] D. B. McCormick, *Photochem. Photobiol.* **1977**, *26*, 169 – 182.
[12] a) J. R. Lakowicz, *Principles of Fluorescence Spectroscopy*, 3rd ed., Springer, Singapore, **2006**, chapters 4 and 10; b) J. T. Vivian, P. R. Callis, *Biophys. J.* **2001**, *80*, 2093 – 2109.
[13] a) P. J. Steinbach, R. Ionescu, C. R. Matthews, *Biophys. J.* **2002**, *82*, 2244 – 2255; b) P. J. Steinbach, *Anal. Biochem.* **2012**, *427*, 102 – 105.
[14] E. Alarcón, A. M. Edwards, A. Aspee, F. E. Moran, C. D. Borsarelli, E. A. Lissi, D. Gonzalez-Nilo, H. Poblete, J. C. Scaiano, *Photochem. Photobiol. Sci.* **2010**, *9*, 93 – 102.
[15] a) M. V. Martin, G. T. Ruiz, M. C. Gonzalez, C. D. Borsarelli, D. O. Martire, *Photochem. Photobiol.* **2012**, *88*, 810 – 815; b) L. Valle, F. E. M. Vieyra, C. D. Borsarelli, *Photochem. Photobiol. Sci.* **2012**, *11*, 1051 – 1061.
[16] a) H. Görner, *J. Photochem. Photobiol. B* **2007**, *87*, 73 – 80; b) P. F. Heelis, B. J. Parsons, G. O. Phillips, J. F. McKellar, *Photochem. Photobiol.* **1979**, *30*, 343 – 347.
[17] E. Alarcón, A. M. Edwards, A. Aspee, C. D. Borsarelli, E. A. Lissi, *Photochem. Photobiol. Sci.* **2009**, *8*, 933 – 943.
[18] M. B. Espeche Turbay, V. Rey, N. M. Argañaraz, F. E. Morán Vieyra, A. Aspée, E. A. Lissi, C. D. Borsarelli, *J. Photochem. Photobiol. B* **2014**, *141*, 275 – 282.
[19] P. F. Heelis in *Chemistry and Biochemistry of Flavoenzymes, Vol. I* (Ed.: F. Mueller), CRC Press, Boca Raton, **1991**, p. 171.
[20] J. Baier, T. Maisch, M. Maier, E. Engel, M. Landthaler, W. Bäumler, *Biophys. J.* **2006**, *91*, 1452 – 1459.
[21] E. A. Lissi, M. V. Encinas, E. Lemp, M. A. Rubio, *Chem. Rev.* **1993**, *93*, 699 – 723.
[22] R. L. Jensen, J. Arnbjerg, P. R. Ogilby, *J. Am. Chem. Soc.* **2012**, *134*, 9820 – 9826.
[23] Y. Fukunaga, Y. Katsuragi, T. Izumi, F. Sakiyama, *J. Biochem.* **1982**, *92*, 129 – 141.
[24] a) P. A. W. van den Berg, K. A. Feenstra, A. E. Mark, H. J. C. Berendsen, A. Visser, *J. Phys. Chem. B* **2002**, *106*, 8858 – 8869; b) G. F. Li, K. D. Glusac, *J. Phys. Chem. B* **2009**, *113*, 9059 – 9061.
[25] a) A. Karen, N. Ikeda, N. Mataga, F. Tanaka, *Photochem. Photobiol.* **1983**, *37*, 495 – 502; b) A. Karen, M. T. Sawada, F. Tanaka, N. Mataga, *Photochem. Photobiol.* **1987**, *45*, 49 – 53.
[26] N. Mataga, H. Chosrowjan, Y. Shibata, F. Tanaka, *J. Phys. Chem. B* **1998**, *102*, 7081 – 7084.
[27] Y. K. Reshetnyak, Y. Koshevnik, E. A. Burstein, *Biophys. J.* **2001**, *81*, 1735 – 1758.
[28] S. D. Black, D. R. Mould, *Anal. Biochem.* **1991**, *193*, 72 – 82.
[29] E. Gasteiger, C. Hoogland, A. Gattiker, S. Duvaud, M. R. Wilkins, R. D. Appel, A. Bairoch in *The Proteomics Protocols Handbook* (Ed.: J. M. Walker), Humana Press, Totowa, **2005**, pp. 571 – 607.
[30] C. D. Borsarelli, S. G. Bertolotti, C. M. Previtali, *Photochem. Photobiol.* **2001**, *73*, 97 – 104.
[31] M. R. Eftink, L. A. Selvidge, P. R. Callis, A. A. Rehms, *J. Phys. Chem.* **1990**, *94*, 3469 – 3479.
[32] J. Yguerabide, H. F. Epstein, L. Stryer, *J. Mol. Biol.* **1970**, *51*, 573 – 590.
[33] F. Wilkinson, *Pure Appl. Chem.* **1997**, *69*, 851 – 856.
[34] R. Ruiz-González, A. L. Cortajarena, S. H. Mejias, M. Agut, S. Nonell, C. Flors, *J. Am. Chem. Soc.* **2013**, *135*, 9564 – 9567.
[35] Y. B. Qi, E. J. Garren, X. Shu, R. Y. Tsien, Y. Jin, *Proc. Natl. Acad. Sci. USA* **2012**, *109*, 7499 – 7504.
[36] D. I. Pattison, A. S. Rahmanto, M. J. Davies, *Photochem. Photobiol. Sci.* **2012**, *11*, 38 – 53.
[37] C. Bittel, L. C. Tabares, M. Armesto, N. Carrillo, N. Cortez, *FEBS Lett.* **2003**, *553*, 408 – 412.
[38] J. M. Villegas, L. Valle, F. E. Morán Vieyra, M. R. Rintoul, C. D. Borsarelli, V. A. Rapisarda, *Biochim. Biophys. Acta, Proteins Proteomics* **2014**, *1844*, 576 – 584.
[39] C. D. Borsarelli, M. Mischne, A. La Venia, F. E. Moran Vieyra, *Photochem. Photobiol.* **2007**, *83*, 1313 – 1318.

Received: October 30, 2014
Published online on ■■ ■■, 2014

A little more sensitivity: C-terminal scission or site-specific mutation of *Rhodobacter capsulatus* ferredoxin–NADP(H) reductase (*Rc*FPR) prevents the charge-transfer quenching of ^{1}FAD* by the conserved Tyr66, producing enhancement of the excited singlet- and triplet-state properties of FAD. This in turn drives the photosensitization of $^1O_2$, challenging the photostability and hence the functionality of the redox flavoprotein.

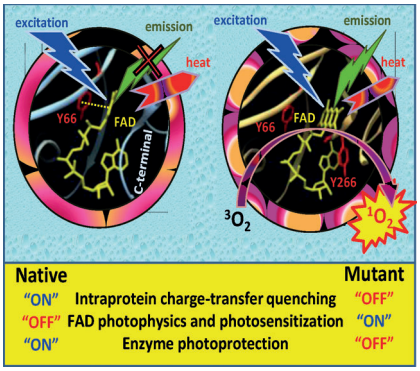

L. Valle, I. Abatedaga, F. E. M. Vieyra, A. Bortolotti, N. Cortez, C. D. Borsarelli**

■■ – ■■

Enhancement of Photophysical and Photosensitizing Properties of Flavin Adenine Dinucleotide by Mutagenesis of the C-Terminal Extension of a Bacterial Flavodoxin Reductase